Available online at www.sciencedirect.com

ScienceDirect

Materials Today: Proceedings 16 (2019) 2273–2279

materialstoday: PROCEEDINGS

www.materialstoday.com/proceedings

Bio-CAM 2017

Highly stable symmetric supercapacitor from cysteamine functionalized multi-walled carbon nanotubes operating in a wide potential window

Gomaa A. M. Ali [a,b,*], Hamidreza Sadegh [c], Mashitah M.Yusoff [a], Kwok Feng Chong [a,*]

[a] *Faculty of Industrial Sciences and Technology, Universiti Malaysia Pahang, Gambang, 26300 Kuantan, Malaysia*
[b] *Chemistry Department, Faculty of Science, Al–Azhar University, Assiut, 71524, Egypt*
[c] *West Pomeranian University of Technology, Szczecin; Faculty of Chemical Technology and Engineering; Institute of Inorganic Chemical Technology and Environment Engineering; ul. Pułaskiego 10, 70-322 Szczecin, Poland*

Abstract

In this paper, the functionalized multi-walled carbon nanotubes with thiol group (MWCNTs-SH) were used to fabricate a symmetric supercapacitor. The symmetric supercapacitor shows a superior electrochemical performance under a wide range of operating voltage up to 2 V and gives a specific capacitance of 85.3 F g^{-1} at 0.25 A g^{-1} (2 V) in 1 M Na_2SO_4. In addition, the supercapacitor shows high energy density of 11.9 Wh kg^{-1}. The findings reveal that this functionalized material is a good candidate for supercapacitor electrode materials.

Selection and/or Peer-review under responsibility of Biomedical and Advanced Materials (Biocam 2017).

Keywords: Cysteamine; EDLC; Functionalization; MWCNTs; Supercapacitors.

1. Introduction

Carbon nanotubes (CNTs) is a promising material as it has high length-to-diameter and surface area–to–volume aspect ratios [1]. It also possesses superior mechanical, thermal, electrical, chemical and thermal properties as well as it has unique internal structures and low mass density [2]. Hence, CNTs have received considerable attention for usage in chemistry and environmental remediation. CNTs could be prepared via different chemical and mechanical method such as; arc–discharge [3], laser vaporization [4], chemical vapor deposition [5], spray–pyrolysis [6], flame

* Corresponding author. Tel.: +6095492403 / Fax: +6095492766.
E-mail address: ckfeng@ump.edu.my, gomaasanad@azhar.edu.eg

Selection and/or Peer-review under responsibility of Biomedical and Advanced Materials (Biocam 2017).

pyrolysis [7]. Single-walled carbon nanotubes (SWCNTs) and multi-walled carbon nanotubes (MWCNTs) are the main two subcategories of CNTs [8, 9]. In addition, there are some other rare types such as double-walled carbon nanotubes (DWCNTs), fullerite, torus and nanoknot [10].

Functionalization is an efficient way of modification processes of the CNTS and it is divided into two main categories: covalent and non–covalent. Surface functional groups modify the surface charge, functionality and reactivity of the surface, hence increase the stability and dispensability of different materials [11]. Numerous studies have been conducted on functionalization of CNTs with different oxygen, nitrogen and sulfur containing groups such as carboxylic, amine, thiol, sulfonic, quinone, ether and hydroxyl [12]. Thiols are high reactive nucleophilic reagents and perfect ligands because of their strong affinity to various heavy metal ions as a result of Lewis acid-base interactions [13]. Cysteamine ($NH_2CH_2CH_2SH$) is an aminothiol and one of the simplest molecules able to bond through its sulfur and nitrogen atoms and a prerequisite for the design of compact monolayers with acceptable properties [14].

Many forms of carbon-based materials are widely used as supercapacitor electrode including graphene, carbon nanoparticles, carbon nanospheres, C60, SWCNTs, DWCNTs, and MWCNTs [15-20]. Carbon materials undergo to elctrodouble layer (EDL) mechanism in storing the charge on the surface of the electrode. On the other hand, metal oxide and conducting polymers undergo a faradic process through redox reactions of the electrode materials [21-24]. CNTs are good candidates for supercapacitor application as they have a good electrical conductivity in addition to its porous structure. The electrochemical performance of CNTs could be enhanced by chemical activation or functionalization. Therefore, introducing new heteroatoms like oxygen, hydrogen, nitrogen and sulfur into the carbon network could enhance the capacitance based on the pseudo effect of these atoms [25].

In this study, functionalized MWCNTs with a carboxyl group and thiol-derivatized was used to fabricate and evaluate the energy storage capabilities. The electrochemical characteristics were studied using cyclic voltammetry (CV) and galvanostatic charge-discharge (CDC).

2. Experimental

2.1. Materials Preparation

The materials used for purification, oxidation and cystamine functionalization of MWCNTs were listed in our previous study [26] and the preparation method was discussed in details. A simple schematic diagram of the synthesis of the process is illustrated in Fig. 1.

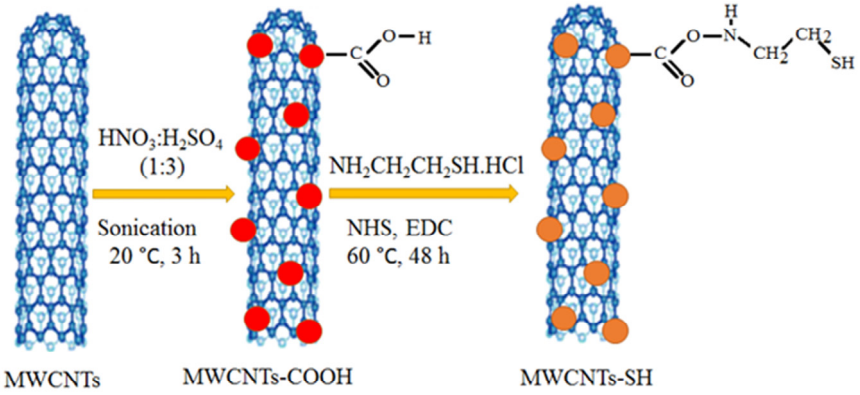

Fig. 1. Schematic diagram shows the surface oxidation and thiol functionalization stages of the functionalization process.

2.2. Materials Characterization

X-ray powder diffraction (XRD), Fourier-transform infrared (FTIR) spectra, Thermogravimetric analysis (TGA) and scanning electron microscope (SEM), N_2 adsorption-desorption and X-ray photoelectron spectrometer (XPS) were performed and the results were discussed in our previous papers [17, 26]. The UV-Vis absorption spectra were measured in the wavelength range from 200 to 900 nm at room temperature using a THERMO SCIENTIFIC UV–Vis spectrophotometer. Measurements were made by suspending about 5 mg of sample in 50 mL dimethylformamide (DMF).

2.3. Electrochemical Measurements

For electrochemical measurements, the electrodes were prepared by the same method discussed in our previous work [17]. Here the electrode was further tested using three-electrode system with the active material as a working electrode, Ag/AgCl as a reference electrode and Pt wire as a counter electrode. In addition, two-electrode system (coin cell design) under different potential windows. The data were collected using an Autolab (PGSTAT M101) electrochemical workstation equipped with frequency response analyzer.

3. Results and Discussion

3.1. Structural and Morphological Properties

The phase analysis using XRD of MWCNTs–COOH and MWCNTs–SH revealed that presence of the hexagonal graphite structure. The functional groups (C=C, C=O, C–O, C–H, O–H and S–H) at each step in the chemical fictionalization have been identified using FTIR. The TGA results provide a quantitative evaluation of the degree of surface functionalization. As expected, the weight loss of MWCNTs, MWCNTs–COOH and MWCNTs–SH was 2.5, 7 and 19% respectively, of the total weight at 600 ºC. SEM data presented in our previous work [17] confirms the thin layer formation of organic compounds on the surfaces of MWCNTs–COOH and MWCNTs–SH. Specific surface area values of MWCNTs, MWCNTs-COOH and MWCNTs-SH were found to be 26.3, 85.9, 94.9 $m^2 g^{-1}$, respectively. The detailed discussion of characterization data was reported elsewhere [17, 26]. Further insights into the electronic conjugation of the prepared materials could be obtained from UV–Vis absorption spectra as shown in Fig. 2.

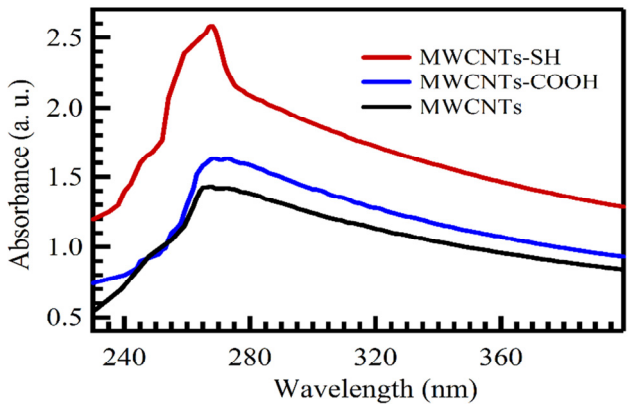

Fig. 2. UV–Vis spectra the indicated materials.

The absorption peak located at 268 nm is corresponding to π/π* transitions of carbon electrons. The adsorption peak of MWCNTs is slightly shifted to lower wavelengths after functionalization with COOH and SH groups. The increasing in adsorption intensity (area under the spectrum line) is an indication of the increase of the dispersion of the material in the DMF [27].

3.3 Electrochemical properties

Fig. 3(a) and (b) shows the CV curves for MWCNTs–SH electrode in the voltage range of -1-0 V and 0-1 V, respectively, in 1 M Na_2SO_4. In both voltage windows, the material exhibits almost rectangular shape without any obvious redox peaks indicating that the charge accumulated on the electrode surface via EDL mechanism. On the other hand, the CDC curves MWCNTs–SH electrode at different current densities are shown in Fig. 3(c). It is clear that the CDC curves are linear with small iR drop. The specific capacitance was calculated from the slope of the discharge curves and presented in Fig. 4(c) as a function of current density. MWCNTs–SH electrode shows a specific capacitance of 68.5 F g^{-1} at 0.25 A g^{-1} and it decreases with an increase in current density to reach 24 F g^{-1} at 2 A g^{-1}. These values are higher than those obtained for CNTs prepared by cut–paste method [28]. Based on these findings MWCNTs–SH has been selected for further electrochemical studies.

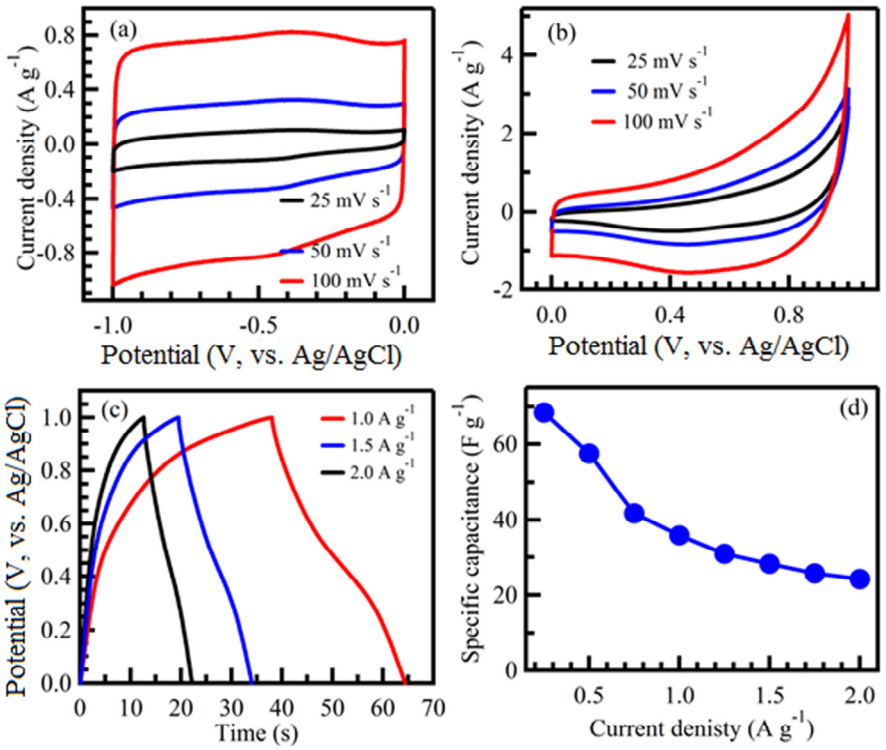

Fig. 3. CV curves at different scan rates in the operating voltage range (a) -1-0 V; (b) 0-1 V; (c) CDC curves at different current densities; (d) the specific capacitance as a function of current density for MWCNTs–SH electrode.

The energy stored in a supercapacitor is directly proportional to the capacitance and the square of operating voltage, therefore increasing the operating voltage of supercapacitors is highly crucial [29]. Generally, the working potential window is limited by the nature of the electrode material and the stability potential and pH of the electrolytes [30]. It is known that, in Na_2SO_4 solution, it can work in the range from -1 to 1 V, and accordingly, the

full cell can work up to 2 V. For this purpose the symmetric supercapacitor was fabricated to investigate the potential window stability and to apply under wider voltages.

Fig. 4(a-c) shows CV curves in 1 M Na_2SO_4 in the potential range of 0–1 V, 0-1.6 and 0–2 V, respectively, at different scan rates of MWCNTs–SH symmetric supercapacitor. Meanwhile, the symmetric supercapacitor shows a wider operating potential range up to 2 V with rectangular CV shapes in all potential windows indicating that it could be applied to higher potentials and storage more energy. In addition, the specific capacitance values were calculated from the area under the CV curves and showed that with increasing the potential window the supercapacitor can store more charge.

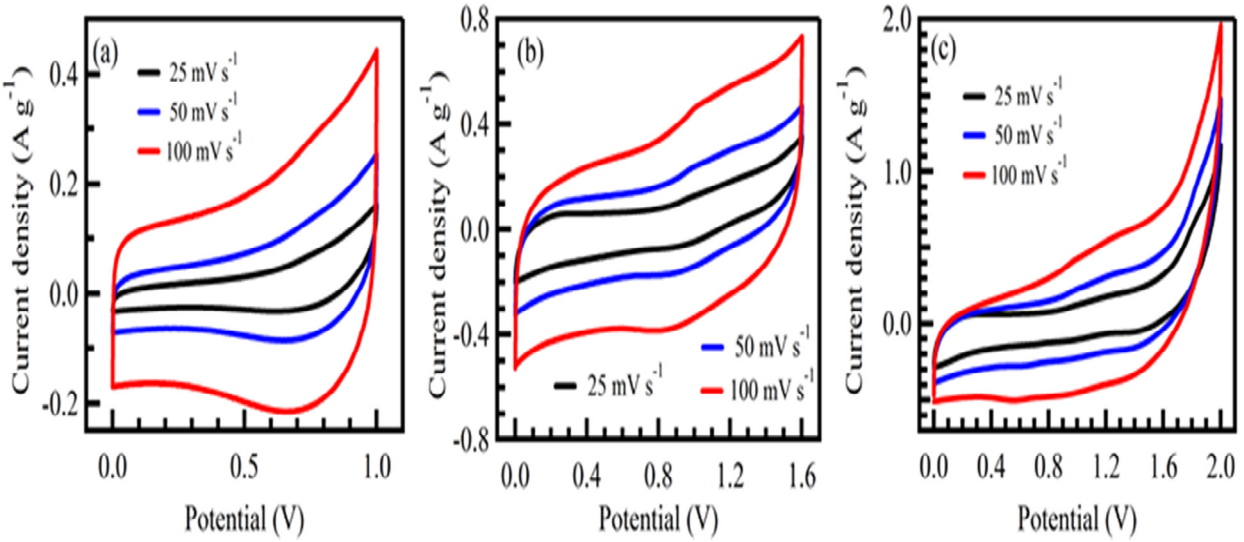

Fig. 4. CV curves at different scan rates in the operating voltage range (a) 0–1 V; (b) 0–1.6 V and (c) 0–2 V as a function of scan rate at different operating voltages for the symmetrical supercapacitor.

On the other hand, It is known that the electrochemical properties directly depend on the morphological characteristics. Fig. 5 (a) shows the CDC curve of the indicated symmetrical supercapacitor at 0.1 A g^{-1}, MWCNTs-SH symmetrical supercapacitor shows the longest discharge time indicating the highest capacitance. The surface area dependence electrochemical properties is shown in Fig 5 (b).

It is found that the specific capacitance linearly depends on the specific surface area (R^2 = 0.8403). This is a result of increasing of the porosity which enhances the movement of the ions through the electrode material particles. The operating voltage window stability of the symmetric supercapacitor was further tested by galvanostatic CDC.

Fig. 5 (c) and (d) shows the CDC curves in different potential windows for MWCNTs-SH symmetrical supercapacitor. Linear charge and discharge curves with very small iR drop are obtained, which indicates that the electrodes have a low internal resistance which leads to better EDL performance.

Moreover, as shown in Fig. 5 (e), the specific capacitance was found to be 85.3, 27.5 and 22.9 F g^{-1} at 0.25 A g^{-1} for 2, 1.6 and 1 V, respectively. Fig. 5 (e) shows the increment of specific capacitance values with increasing voltage window. This high specific capacitance is a result of pseudocapacitance contribution due to the presence of thiol groups [17]. In addition, the Ragone plot is shown in Fig. 5 (f), where the MWCNTs-SH symmetrical supercapacitor shows energy density of 11.9 W h kg^{-1} at a power density of 277.8 W kg^{-1}.

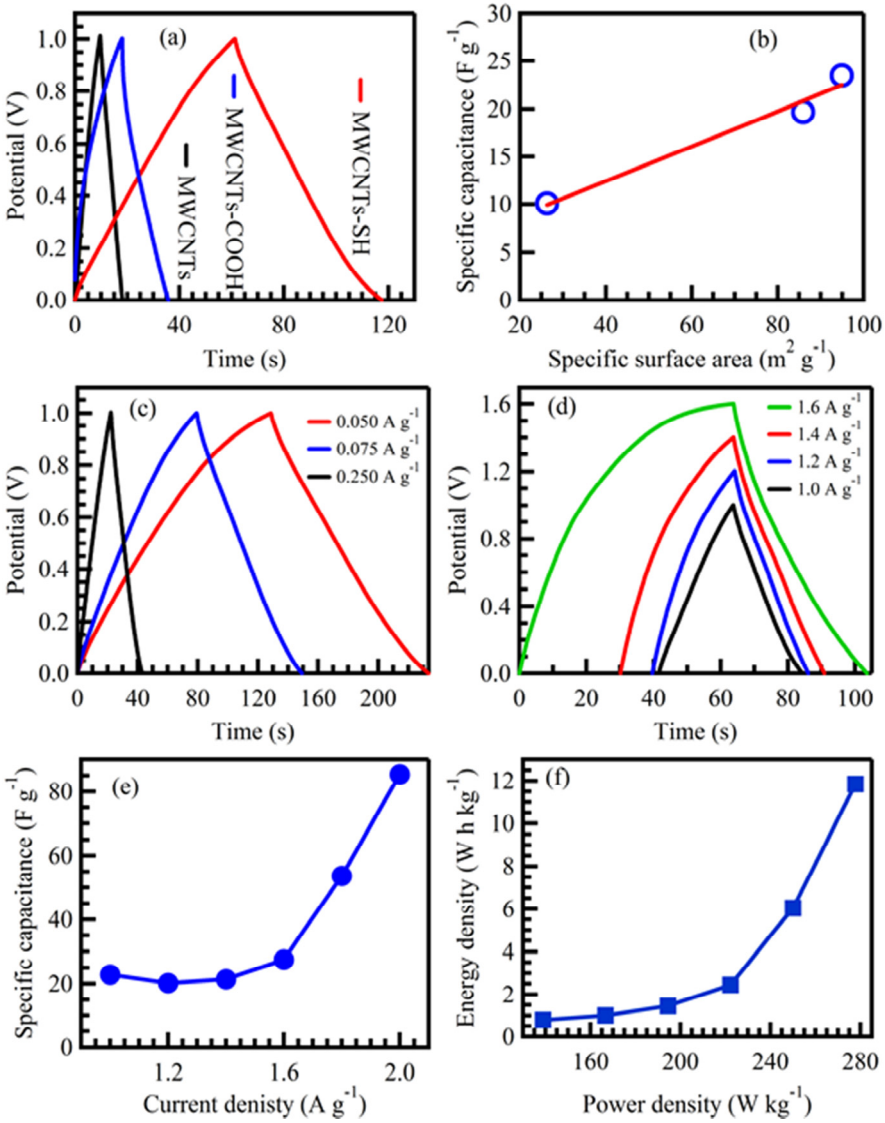

Fig. 5. (a) CDC curves at 0.1 A g^{-1} for the indicated supercapacitors; (b) specific capacitance as a function of specific surface area; CDC curves at different current densities in the range of (c) 0–1 V; (d) at 0.25 A g^{-1} at different operating voltages; (e) the specific capacitance as a function of operating voltage; (f) Ragone plot for the symmetrical supercapacitor.

4. Conclusions

The practical symmetrical supercapacitor from MWCNTs–SH was tested for supercapacitor application and showed excellent EDL behavior in 1 M Na_2SO_4 solution. MWCNTs–SH showed high specific capacitance of 85.3 F g^{-1} under a wide range of operating voltage (0–2V). The practical supercapacitor shows high energy density of 11.9 W h kg^{-1}. The findings reveal that this functionalized material is a promising material for supercapacitor applications

Acknowledgments

This work was supported by Ministry of Education Malaysia FRGS [RDU160118: FRGS/1/2016/STG07/UMP/02/3] and Universiti Malaysia Pahang [grant number RDU170357].

References

[1] R.K. Abu Al–Rub, A.I. Ashour, B.M. Tyson, Constr. Build. Mater. 35 (2012) 647–655.
[2] M. Mahmoodi, M. Arjmand, U. Sundararaj, S. Park, Carbon 50 (2012) 1455–1464.
[3] S. Iijima, Nature 354 (1991) 56-58.
[4] A. Thess, R. Lee, P. Nikolaev, H. Dai, P. Petit, J. Robert, C. Xu, Y.H. Lee, S.G. Kim, A.G. Rinzler, Science 273 (1996) 483–487.
[5] R.J. Cartwright, S. Esconjauregui, R.S. Weatherup, D. Hardeman, Y. Guo, E. Wright, D. Oakes, S. Hofmann, J. Robertson, Carbon 75 (2014) 327–334.
[6] Z. Sarkozi, K. Kertesz, A.A. Koos, Z. Osvath, L. Tapaszto, Z.E. Horvath, P. Nemes-Incze, I.Z. Jenei, Z. Vertesy, N.S. Daroczi, A. Darabont, O. Pana, L.P. Biro, J. Optoelectron. Adv. Mater. 10 (2008) 2307–2310.
[7] B.M. Sun, W.H. Cao, Y.H. Guo, Y. Wang, J.T. Luo, P. Jiang, AIP Adv. 3 (2013) 092102–092109.
[8] F. Avilés, J. Cauich-Rodríguez, L. Moo–Tah, A. May–Pat, R. Vargas–Coronado, Carbon 47 (2009) 2970–2975.
[9] Z. Liu, Z. Shen, T. Zhu, S. Hou, L. Ying, Z. Shi, Z. Gu, Langmuir 16 (2000) 3569–3573.
[10] A. Aqel, K.M.M.A. El-Nour, R.A.A. Ammar, A. Al–Warthan, Arabian J. Chem. 5 (2012) 1–23.
[11] H. Sadegh, R. Shahryari–ghoshekandi, S. Agarwal, I. Tyagi, M. Asif, V.K. Gupta, J. Mol. Liq. 206 (2015) 151–158.
[12] S.K. Park, Q. Mahmood, H.S. Park, Nanoscale 5 (2013) 12304–12309.
[13] E.F. Vieira, J.d.A. Simoni, C. Airoldi, J. Mater. Chem. 7 (1997) 2249–2252.
[14] S. Bloxham, O. Eicher–Lorka, R. Jakubėnas, G. Niaura, Spectrosc. Lett. 36 (2003) 211–226.
[15] E. Frackowiak, K. Metenier, V. Bertagna, F. Beguin, Appl. Phys. Lett. 77 (2000) 2421–2423.
[16] G.A.M. Ali, S.A. Makhlouf, M.M. Yusoff, K.F. Chong, Rev. Adv. Mater. Sci. 41 (2015) 35–43.
[17] G.A.M. Ali, E.Y. Lih Teo, E.A.A. Aboelazm, H. Sadegh, A.O.H. Memar, R. Shahryari-Ghoshekandi, K.F. Chong, Mater. Chem. Phys. 197 (2017) 100-104.
[18] G.A.M. Ali, S.A.A. Manaf, D. A, K.F. Chong, G. Hegde, J. Energy Chem. (2016).
[19] G. Hegde, S.A. Abdul Manaf, A. Kumar, G.A.M. Ali, K.F. Chong, Z. Ngaini, K.V. Sharma, ACS Sustainable Chem. Eng. 3 (2015) 2247−2253.
[20] G.A.M. Ali, S.A.B.A. Manaf, A. Kumar, K.F. Chong, G. Hegde, J. Phys. D: Appl. Phys. 47 (2014) 495307–495313.
[21] G.A.M. Ali, O.A. Fouad, S.A. Makhlouf, M.M. Yusoff, K.F. Chong, J. Solid State Electrochem. 18 (2014) 2505–2512.
[22] G.A.M. Ali, L.L. Tan, R. Jose, M.M. Yusoff, K.F. Chong, Mater. Res. Bull. 60 (2014) 5–9.
[23] G.A.M. Ali, O.A.G. Wahba, A.M. Hassan, O.A. Fouad, K.F. Chong, Ceram. Int. 41 (2015) 8230–8234.
[24] G.A.M. Ali, M.M. Yusoff, Y.H. Ng, N.H. Lim, K.F. Chong, Curr. Appl Phys. 15 (2015) 1143–1147.
[25] G. Lota, K. Fic, E. Frackowiak, Energy Environ. Sci. 4 (2011) 1592–1605.
[26] H. Sadegh, K. Zare, B. Maazinejad, R. Shahryari-ghoshekandi, I. Tyagi, S. Agarwal, V.K. Gupta, J. Mol. Liq. 215 (2016) 221-228.
[27] E.C. Botelho, E.R. Edwards, B. Bittmann, T. Burkhart, J. Braz. Chem. Soc. 22 (2011) 2040–2047.
[28] H. Zhang, G.P. Cao, Y.S. Yang, Nanotechnol. 18 (2007) 195607–195611.
[29] G.A.M. Ali, A. Divyashree, S. Supriya, K.F. Chong, A.S. Ethiraj, M. Reddy, H. Algarni, G. Hegde, Dalton Trans. 46 (2017) 14034-14044.
[30] F. Hekmat, B. Sohrabi, M. Rahmanifar, M. Vaezi, J. Mater. Chem., A 2 (2014) 17446-17453.